scientific reports

Check for updates

OPEN

A portable multi-taxa phenotyping device to retrieve physiological performance traits

Hadley England[1]✉, Andrei Herdean[1], Jennifer Matthews[1], David J. Hughes[2], Christine D. Roper[1], David J. Suggett[1,3], Christian R. Voolstra[4] & Emma F. Camp[1]✉

Organismal phenotyping to identify fitness traits is transforming our understanding of adaptive responses and ecological interactions of species within changing environments. Here we present a portable Multi-Taxa Phenotyping (MTP) system that can retrieve a suite of metabolic and photophysiological parameter across light, temperature, and/or chemical gradients, using real time bio-optical (oxygen and chlorophyll *a* fluorescence) measurements. The MTP system integrates three well-established technologies for the first time: an imaging Pulse Amplitude Modulated (PAM) chlorophyll *a* fluorometer, custom-designed well plates equipped with optical oxygen sensors, and a thermocycler. We demonstrate the ability of the MTP system to distinguish phenotypic performance characteristics of diverse aquatic taxa spanning corals, mangroves and algae based on metabolic parameters and Photosystem II dynamics, in a high-throughput capacity and accounting for interactions of different environmental gradients on performance. Extracted metrics from the MTP system can not only provide information on the performance of aquatic taxa exposed to differing environmental gradients, but also provide predicted phenotypic responses of key aquatic organisms to environmental change. Further work validating how rapid phenotyping tools such as the MTP system predict phenotypic responses to long term environmental changes in situ are urgently required to best inform how these tools can support management efforts.

Photosynthetic organisms underpin the health and functioning of aquatic ecosystems and are increasingly vulnerable to the impacts of climate change[1,2]. Understanding the intricate interactions between multiple stressors and their effects on the physiological performance of photosynthetic organisms is crucial for predicting their fitness trajectory, survival, and distribution[3,4], and in turn the effective management of marine systems. While molecular[5] and chemical[6] biomarkers can be used, phenotyping by identifying the expression of photosynthetic traits[7] possesses a unique advantage that allows use of direct and non-intrusive fluorescence-based metrics[8–10]. Measurement of chlorophyll *a* fluorescence via active induction protocols has become the standard approach to assess the physiological state and fitness of photosynthetic taxa[8,9,11] in aquatic systems[12]. Most biological pathways of these organisms directly or indirectly depend on photosynthesis as the vast majority of their metabolic requirements are fulfilled through primary production; as such, derived chlorophyll *a* fluorescence parameters can broadly inform organism physiology beyond operation of the photosynthetic machinery[13,14]. In cases where photosynthetic organisms exist in symbiotic relationships with heterotrophs (e.g., spanning bacteria to invertebrates), employing parallel techniques such as respirometry and chlorophyll *a* fluorescence measurements can be critical to inform complementary fitness traits across multi-taxa partnerships where host metabolism can act discretely from symbiont photophysiology.

Modern aquatic physiological phenotyping tools offer a diverse array of metrics to assess metabolic performance in different environments[8,10,14]. Common tools include single-turnover and multi-turnover fluorometry protocols[9,10], but also hyperspectral imaging[15] and oxygen (O_2) analysis[16]. Phenotyping techniques have been applied in aquatic systems at scales from single cells[14,17,18] through to entire metazoan individuals[8]. However, high-throughput, multi-analytical phenotyping technology for assessment of organisms within terrestrial systems is far more advanced[19], where rapid on-site phenotyping systems are transforming agriculture practices[20];

[1]University of Technology Sydney, Climate Change Cluster, Ultimo, NSW 2007, Australia. [2]National Sea Simulator, Australian Institute of Marine Science, Townsville, QLD, Australia. [3]KAUST Reefscape Restoration Initiative (KRRI) and Red Sea Research Center (RSRC), King Abdullah University of Science and Technology, 23955 Thuwal, Saudi Arabia. [4]Department of Biology, University of Konstanz, Constance, Germany. ✉email: hadley.england@student.uts.edu.au; emma.camp@uts.edu.au

for example, through the identification and selection of water stress tolerant individuals[21]. Recently, a "Coral Bleaching Automated Stress System" (CBASS)[22,23] was developed to determine thermal thresholds and prospective recovery capacity—both considered key traits (and hence phenotypes)—within an 18-h period across four distinct thermal cycling profiles, demonstrating high efficacy in resolving differences in coral thermal tolerance[24]. Beyond the CBASS, however, portable, high-throughput multi-parameter technologies for field assessment of aquatic organisms is lacking. In this work, we address this need by introducing a high-throughput portable phenotyping device that can assess performance of diverse aquatic photosynthetic organisms (algae[13,17] to holobiont individual[25]).

Our Multi-Taxa Phenotyping (MTP) system advances a previously described system designed for analysing phenotypes in microalgal cultures using a 96-well plate[13]. The MTP system integrates three well-established technologies for the first time: an imaging Pulse Amplitude Modulated (PAM) chlorophyll *a* fluorometer, custom-designed well plates equipped with optical O_2 sensors, and a thermocycler. This innovative combination is facilitated by an adaptor plate and incorporates customised data acquisition and processing protocols. Collectively the MTP system integrates respirometry metrics with fluorometry-based Photosystem II (PSII) dynamics allowing for a physiological assessment of both partial and entire organisms, thereby broadening application to holobiont (or metaorganism) phenotyping. Having tools that can provide rapid, real-time, informed decision-making based on observable phenotypic responses to multiple environmental stressors, such as temperature, nutrients, and light[8] will aid management and conservation of aquatic ecosystems by enabling the identification and selection of resilient individuals that can be utilised in restoration and protection activities[26].

Methods

A Pulse Amplitude Modulation (PAM) imaging fluorometer (Open FluorCam FC 800-O/1010, Photon Systems Instruments, Brno, Czech Republic) fitted with an 8 mm, f/1.4 Manual Iris C-mount lens (VST America, Arlington Heights, IL, U.S.A.) capable of detecting wavelengths 610–780 nm was positioned above a gradient-capable thermocycler (ABI Veriti, Applied Biosystems, Waltham, MA, USA; Fig. 1a). The thermocycler was set so that discrete wells were subjected to different temperatures across a user defined gradient (Fig. 1b) or held at a single temperature (Fig. 1c) depending on the user defined Protocol (see below). Broad spectrum white light was provided by an array of LEDs positioned at a 25° angle and 30 cm distance relative to the MTP sample plate (Fig. 1; Supplementary Fig. 1). To integrate the imaging PAM, sample plate and thermocycler for the MTP system, a custom-made adaptor plate was required.

MTP adapter plate To integrate the thermocycler into the MTP system, a custom-designed adapter plate was manufactured at the University of Technology Sydney using Rigid 10 K resin and printed with a Form 2 Desktop SLA printer (Formlabs, Somerville, MA, U.S.A.; Fig. 1a). The modified adapter plate was used to transform a standard 96-well plate into a 24-well plate, combining four adjacent wells with a size of 14 × 14 × 9 mm. Samples of up to 12 × 12 × 8 mm can be adequately contained (Fig. 1), enabling assessment of diverse taxa. A Styrofoam insulation ring was applied around the adapter plate to achieve replicable temperatures (see Supplementary Fig. 2). The adapter plate was securely attached to the well plate using super glue (Gorilla Glue, Cincinnati, OH, U.S.A.) to ensure watertight conditions. A 2 mm tempered glass sheet, measuring 113–78 mm (Huizhou Konshen Glass Co., Huizhou, Guangdong, China) was recessed within the plate and secured by a custom 3D printed flexible plastic seal (Flexible 80A resin), creating a watertight seal for the plate as well as a mounting surface for the optical O_2 sensors (Supplementary Fig. 1). The use of this watertight adapter plate also allowed different chemical gradients to be assessed[13] (Supplementary Fig. 3). Optical O_2 sensors (OXSP5, Pyroscience, Aachen, Germany), with a diameter of 5 mm, were positioned on the underside of the glass lid using clear silicon (All Clear, Selleys, Padstow Australia). These sensors use fluorescence quenching to measure O_2 concentrations and can be directly read by a PAM imaging fluorometer as they utilise an excitation wavelength range of 610–640 nm and an emission wavelength range of 760–790 nm.

Taxa were placed into the wells of the adapter plate, ensuring each sample was not placed directly underneath the O_2 sensor positioned in the corner of each well. The wells were then topped up with seawater to overflowing. The glass lid was then placed on one side and lowered down at an angle and the plastic seal placed around the outside, thus securing the lid to create a watertight seal with no air bubbles trapped inside the well plate (Supplementary Fig. 1). When samples were placed in the adaptor plate for O_2 assessment, the plate was filled with 0.2 µm filtered seawater to limit any microbial respiration. Once the adaptor plate was inserted into the thermocycler, one of two protocols were initiated.

Protocol 1—a multistage dynamic photophysiological response protocol was developed as a custom PAM Protocol with 3 stages of performance metric retrieval that collectively considered the pre- and post-stress state, as well as performance across a combination of light and/or temperature stress conditions (see Fig. 1b).

Stage 1—(Fig. 1b; T0 to T1) consisted of 10 min of low light acclimation under 10 µmol photons m^{-2} s^{-1} whilst the thermocycler was set to maintain the sample(s) at growth temperature followed by a measurement acquisition of F_q'/F_m'. This provided an initial sample assessment to determine organism photophysiological state prior to initiation of the temperature and light exposure (Fig. 1b [T0 to T1]; Supplementary Fig. 4).

Stage 2—(Fig. 1b; T1 to T2) consisted of a temperature treatment of the samples under pre-illumination followed by a Rapid Light Curve (RLC). Desired temperatures were then programmed and applied to the thermocycler and samples were maintained at the new temperatures for 10 min. A RLC was then initiated, starting with a measurement acquisition of F_q'/F_m' to characterise the effect of temperature exposure independently of light. A sequence of 15 increasing light intensity (59–1749 µmol photons m^{-2} s^{-1}) steps were applied, with each step applied for 30 s (Supplementary Fig. 5) yielding the total time for stage 2 of 17.5 min. This RLC was used to determine dynamic chlorophyll *a* fluorescence parameters indicative of photosynthetic performance, specifically: the photochemical efficiency of PSII (F_q'/F_m'), non-photochemical quenching (NPQ), maximum relative electron

transport rate ($rETR_{max}$), minimum saturation light intensity (E_K), and the rate of photochemistry in light limiting conditions (α). It was identified that an optimum light step length of 30 s was required to ensure $rETR_{max}$ remained high whilst inducing non-photochemical quenching within the samples (Supplementary Fig. 5).

Stage 3—After the RLC completion, the sample was returned to ambient temperature using the thermocycler. Samples were maintained in this state for 10 min under low light (10 µmol photons m^{-2} s^{-1}) and subjected to a further acquisition of F_q'/F_m' (Figs. 2a, 3a, b). From this final F_q'/F_m' measurement any residual NPQ that did not relax during the 10 min of stage 3 was determined, thereby providing a measure of the slow-relaxing NPQ (including photoinhibition) post photo- and thermal-exposure (Fig. 1b [T2 to T3]). Detailed instrument protocols which include all used settings and time points where the saturation pulses were applied can be accessed online (https://github.com/HadleyEngland/MTP-Protocol-.git).

The thermocycler settings for *Protocol 1* consisted of a 10 min holding period at ambient growth temperature (T0–T1), a 10 min ramping period where the target temperature gradient was achieved, a 7.5 min hold at target temperature (T1–T2) and a further 10 min hold once returned to growth temperature (T2–T3). Well temperatures were measured prior to each experiment to ensure the target temperatures were being achieved using a previously described[17] series of eight micro thermistors (NTC type, EPCOS) connected in a line and controlled by a microprocessor controller (Uno, Arduino Italy). To measure temperature at T2, the glass lid was briefly lifted, and all sensors were quickly placed into the wells. Each well was measured using two sensors with the mean of the two sensors recorded. This process was performed twice in quick succession, each time starting at a different end of the adapter plate to ensure thermal heterogeneity (Supplementary Fig. 2).

Protocol 2—oxygen dynamic response protocol—was designed to assess O_2 dynamics of taxa under both light and dark conditions, and with the capacity to repeat across varying temperatures (Fig. 1c). The initial part of *Protocol 2* involved a 30 min dark respiration period, followed by a subsequent 30 min illumination stage at a predetermined light intensity. The light intensity was ascertained from *Protocol 1* and average E_K values for each species were determined using Hennige et al.[27] (Fig. 2b). After the adapter plate was placed on the thermocycler the temperature was set to ramp and hold the target temperature for 10 min to allow respiration to stabilise and for the thermocycler to reach target temperature. Fluorescence of both the O_2 spot and sample were measured at 3 min intervals utilising an actinic saturating pulse of light, resulting in a total of 20 measurements during both

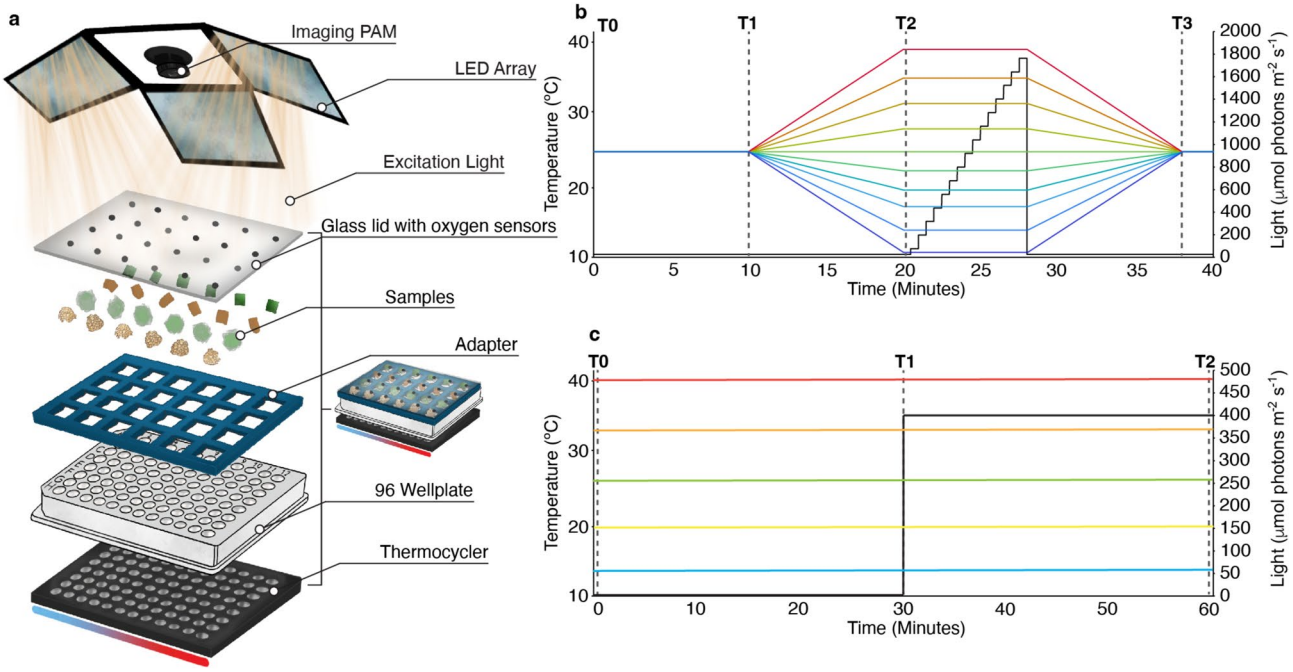

Fig. 1. The Multi-Taxa Phenotyping (MTP) system and protocols. (**a**) Schematic representation showing the MTP system consisting of the fluorometer imaging device (top), plate assembly (centre) and thermocycler (bottom). (**b**) *Protocol 1*—a Multistage Dynamic Photophysiological Response Protocol—showing the temperature treatment profile and sample illumination steps for each stage of the procedure. Coloured lines (blue to red gradient) depict temperature profiles, the black line shows illumination treatment (ranging from 10 to 1749 µmol photons m^{-2} s^{-1}), and dotted lines show the three critical time points (stages) of the protocol. The different segments of the protocol are: T0 to T1 where sample is maintained at its environmental temperature in low light; T1 to T2 represents the start of temperature gradient and acclimation in low light; T2 to T3 is the rapid light curve (RLC) and the subsequent return of the sample temperature back to initial values from T0 at the end of the RLC; T3 is the final measurement point. (**c**) *Protocol 2—Oxygen Dynamic Response Protocol*—used to assess O_2 dynamics of taxa. Black line indicates light intensity and coloured lines represent a range of potential temperatures applied to the adapter plate depending on user requirements. T0 to T1 is the dark phase where respiration is measured and T1 to T2 is the light phase where photosynthesis is measured.

dark and light phases. Changes in fluorescence of the spots during the light and dark periods (with dark values added to the light values to get gross photosynthesis, see Supplementary Fig. 6) were then divided (P_G by R), yielding a photosynthesis (gross, P_G)-to-respiration (P_G:R) ratio (Fig. 4a–c). The rETR of each sample was also derived by averaging the rETR measurements from each 3 min interval (Fig. 4d). This facilitated direct comparison between P_G:R and rETR values, enabling a more detailed evaluation of photochemical capacity. Absolute rates of respiration (R)[28] (Fig. 4e) and gross photosynthesis (P_G; Fig. 4f) were also achieved by calculating the surface area of each coral fragment using ImageJ[29] and carrying out a two-step calibration curve on the optical sensors (Supplementary Fig. 7).

O_2 calibration—Prior to the experiment the glass lid with O_2 sensors was placed into a zip lock bag containing ca. 200 mL of 0.2 µm filtered seawater. An aeration stone was then placed inside the bag and nitrogen was bubbled through the water for 1 h to completely purge dissolved O_2 and create a 0% O_2 seawater solution. After 1 h the air stone was removed, along with any excess nitrogen and the bag sealed tight. The bag containing the glass lid was then placed underneath the imaging PAM where the fluorescence of each individual dot was recorded. The glass lid was then removed, fully dried, and placed under the imaging PAM where another measurement was taken, yielding a 100% O_2 saturated fluorescence reading for each sensor. Using these fluorescence readings as calibration points, the exact O_2 concentrations of each well could then be calculated based on the changes in fluorescence of each sensor over a given time. Returned values were normalised to the corresponding temperature and salinity dependant solubility of O_2[28], as well as sample surface area and incubation time to provide a rate measurement (µg O^2 cm^{-2} h^{-1}) to obtain absolute rates of photosynthesis and respiration across different temperatures.

Multi-taxa application of the MTP system—An initial validation step of the MTP system was to assess whether hypoxic conditions occurred due to the chamber size relative to taxa biomass used. We undertook a series of O_2 drawdown assessments[28] on Scleractinian coral. Coral fragments of varying species (*Pocillopora damicornis* and *Seriatopora hystrix;* sourced from the Great Barrier Reef, Queensland (Great Barrier Reef Aquatics, Cairns)) and biomass (ca. 0.05–0.2 g; Supplementary Fig. 7a,b) were placed in the sample plate and incubated in the dark for 45 min. O_2 drawdown was measured using the optical O_2 sensors (OXSP5, Pyroscience, Aachen, Germany; Supplementary Fig. 7c). The 45 min timeframe was selected as it was double that of the dark period in any of the MTP Protocols, and thus presented a conservative estimate of O_2 depletion within wells of the MTP system. From this validation it was confirmed that no hypoxic or anoxic conditions (e.g., O_2 sustained below 2 mg L^{-1} of O_2[30]) occurred during the Protocols (Supplementary Fig. 7) providing confidence in proceeding with further application of the MTP system.

The MTP system was trialled on multiple taxa. Coral (*Acropora kenti*) was sourced from the Great Barrier Reef, Queensland (Great Barrier Reef Aquatics, Cairns) and maintained at the University of Technology Sydney (UTS) aquarium facility for 6 months under conditions similar to their natural environment[31]. Mangrove leaves (*Avicennia marina*) were sourced from Towra Aquatic reserve Sydney (under permit #P22/001AR-TP and #P20/0027–1.0) and macroalgae (*Ulva lactuca* and *Sargassum verruculosum*) were sourced from Coogee Beach, Sydney (− 33.9215, 151.2585) and stored at the UTS seaweed facility for two days before sampling. As the MTP system was trialled on both temperate and tropical marine taxa, a range of 14–38.6 °C was determined as optimal to retrieve Thermal Performance Curves (Figs. 2, 4). Consequently, the 24-well plate adaptor allowed for six discrete temperatures to be tested simultaneously (Fig. 1). As such, we opted to run the MTP *Protocol 1* twice at two complimentary thermal gradients (14–26 °C and 26–38.6 °C), to populate a higher resolution TPC when testing multiple taxa from broad thermal ranges (Fig. 2). Prior to use, the temperature was mapped in each well to confirm the exact temperature exposure taxa were subjected to. Sampling of all taxa was performed between 11 am and 2 pm to minimise the potential effects of circadian rhythm upon photobiology and metabolism[32]. When sampling *A. kenti*, *A. marina*, *S. verruculosum* or *U. lactuca*, small 8–11 mm samples were taken and placed directly into the sample plate together with 0.2 µm filtered seawater from their respective holding aquaria. Mangrove leaves (*A. marina*) were cut into 10 × 10 mm squares and placed into the wells which were filled with distilled water to alleviate any osmotic stress that could occur from using salt water. Once all samples were loaded into the well plate, the glass lid was placed on top, sealing each well and ensuring no air bubbles were trapped under the glass. The plate was then placed immediately onto the thermocycler and *Protocol 1* was initiated (Fig. 1b).

A further experiment was undertaken on coral to evaluate how phenotypes derived from the MTP system compared to those obtained utilising the commonly applied CBASS[22,23] system, noting the two systems have fundamentally different aspects, such as thermal range, ramping rate and extracted photophysiological parameters. Three genotypes of two coral species (*A. kenti* and *P. damicornis*) sourced from the Great Barrier Reef, Queensland (Great Barrier Reef Aquatics, Cairns) were subjected to both the MTP and CBASS protocols. The CBASS assay entailed an 18-h acute heat stress assay, consisting of a control temperature at 27 °C and three treatments at 30, 33 and 36 °C which were ramped to target temperatures from control over 3 h, held at target temperatures for 3 h, then ramped down over 1 h at which point F_v/F_m values of samples were measured[22,23]. Fragments of the same six genotypes for both coral species were concurrently analysed using the MTP system and *Protocol 1* with the defined temperature range 23.1 °C to 36.4 °C (Fig. 3a–d). F_q'/F_m' results from T3 of *Protocol 1* of the MTP system were chosen to compare with F_v/F_m values from the CBASS assay as they both indicated the efficiency and/or damage to PSII after being exposed to a thermal treatment. To assess how low light pre-illumination affected photochemical efficiency under ambient conditions, an additional test of three coral species, *Montipora capricornis, Montipora digitata* and *A. kenti,* ($n = 8$ per species), was undertaken (Supplementary Table 1).

A final experiment assessed how O_2 dynamics were impacted across a temperature gradient for three coral species (*M. capricornis, M. digitata* and *P. damicornis*; $n = 8$ replicates per species). To do this, the above species were exposed to four distinct temperatures (15, 26, 32 and 35 °C). Relative electron transport rates (rETR; Fig. 4d), respiration (R; Fig. 4e) and gross photosynthesis (P_G; Fig. 4f), as well as P_G to R ratios (P_G:R; Fig. 4a–c; Supplementary Table 2) were calculated using *Protocol 2* of the MTP system.

Data analysis—O_2 dynamics were assessed by one-way Analysis of Variance (ANOVA) and Pearson's Correlation tests conducted in RStudio (RStudio Team (2024) *Boston, MA)* Assumptions of normality and equal variance were met and checked using Shapiro–Wilk and Levene's tests respectively. Photophysiological parameters F_q'/F_m' (T3), $rETR_{max}$ (T2 RLC), residual NPQ (T1–T3), NPQ_{max} (T2 RLC) and α (T2 RLC) were extracted from the fluorescence images using the FluorCam software. Individual wells were selected in post-processing with all excited pixels within them being averaged and analysed. E_K values were calculated using F_q'/F_m' results obtained across the RLC and modelled using an exponential function[27]. Residual NPQ was calculated from F_m (T1) and F_m' (T3; Fig. 1b). Principal Component Analysis plots (PCAs; Fig. 3e,f) were created in Metaboanalyst 5.0 (Canada) using cube root data transformation and auto scaling, incorporating the five above mentioned photophysiological parameters. rETR heatmaps (Fig. 2c) were generated using Origin Pro (Northampton, MA, USA) and data smoothed between temperature points.

Thermal performance curves (TPCs) for $rETR_{max}$ values (Fig. 2d) were derived using the Gaussian model for all four taxa and created using RStudio. For each taxon, four TPCs were created giving an $n = 4$. From each TPC, T-min and T-max were calculated and indicate the points where $rETR_{max}$ drops to 30% of the organisms maximum $rETR_{max}$ value, thus giving both a low and high thermal limit. Using these values, thermal ranges could then be established by subtracting T-min from T-max. T-opt (the optimal temperature at which the maximum relative rate of photosynthetic electron transport is observed) was also calculated from this model for each taxon. ANOVA and Tukey's post-hoc tests were also conducted on outputs from the Gaussian model (Table 1, Supplementary Table 3). Mean α values were plotted and TPCs for each taxon were generated using the Briere model[33,34] (Fig. 2e; $n = 4$ per data point) to retrieve T-opt (the temperature at which the maximum rate of photosynthetic efficiency is seen under light limiting conditions). To establish thermal thresholds for each taxon (Figs. 2f, 3g,h), F_q'/F_m' values from T3 of *Protocol 1* were modelled using a log-logistic regression model in RStudio[22,23] to determine the ED50, defined as the temperature at which observed F_q'/F_m' values from T3 decreased by 50% from the modelled median; in doing so, F_q'/F_m' self-normalises for any variance in magnitude inherent across samples. A Tukey's HSD test was used to compare the photosynthetic efficiency measurements retrieved for corals using the MTP and CBASS methods at 36.5 °C and 35.6 °C respectively (Fig. 3a–d).

Results

Multi-taxa application—We analysed four different taxa, *Acropora kenti* (coral tissue fragment), *Avicennia marina* (mangrove leaf), *Sargassum verruculosum* (brown macroalgae), and *Ulva lactuca* (macroalgal frond) to assess the MTP system's ability to extract temperature dependent photophysiological performance metrics across a range of photosynthetic organisms. Prior to any taxa analysis, repeat MTP runs without any biological test material in the wells demonstrated stability in the temperature of wells, with maximum variation of 0.11 °C across three runs at two different temperatures (15 °C and 32 °C). For the multi-taxa comparison, ED50 values ranged from 37.1 °C for *A. kenti* to 44.3 °C for *A. marina* (Fig. 2f). Modelled TPCs (Fig. 2d; Table 1) based on $rETR_{max}$ yielded T-opt that was highest for *U. lactuca* and lowest for *A. kenti* (Supplementary Table 4). Taxon ranking based on the F_q'/F_m' derived ED50 (Fig. 2f) and $rETR_{max}$ derived T-max values for T2 (Fig. 2d, Table 1) were the same. T-min and T-max were generally distinct between each taxon ($P < 0.01$; Table 1), with thermal range (T-max–T-min) the widest for *A. marina* and narrowest for *S. verruculosum* (Fig. 2d, Table 1, Supplementary Table 4). Thermal range for *A. marina* (23.7 °C) and *U. lactuca* (22.0 °C) was significantly wider than for *A. kenti* (14.9 °C) and *S. verruculosum* (14.5 °C; Tukey HSD < 0.01; Supplementary Table 3). TPCs based on α indicated a range in T-opt of 22.5–30.2 °C, where T-opt was lowest for *A. marina* and highest for *S. verruculosum*. Finally, E_K values for all taxa were highly variable with temperature (Fig. 2b).

MTP and CBASS derived phenotypes—Phenotypic response patterns were similar across both methods, except for *P. damicornis* genotypes 1 and 2 (P1 and P2, Fig. 3g,h) where the MTP but not CBASS extracted a small difference in thermal thresholds. Both methods identified *A. kenti* genotype 2 (A2) and *P. damicornis* genotype 3 (P3) with higher F_v/F_m (CBASS) and F_q'/F_m' (MTP) values than for other genotypes within the same species under thermal stress of 36.5 °C (MTP) and 35.6 °C (CBASS) ($P < 0.05$, Fig. 3a–d, Supplementary Table 5). The MTP further identified A2 and P3 as a distinct grouping together in the 36.5 °C PCA analysis (Fig. 3f) that incorporated a variety of parameters extracted from MTP *Protocol 1* (Fig. 3i–l).

Taxon		rETRmax	T-opt	T-min	T-max	Thermal range
A. kenti		91.0 ± 3.21	24.7 ± 0.20	17.3 ± 0.37	32.2 ± 0.20	14.9 ± 0.43
A. marina		145.0 ± 5.76	26.8 ± 0.93	14.9 ± 1.31	38.7 ± 0.63	23.7 ± 0.87
U. lactuca		95.8 ± 2.40	27.6 ± 0.44	16.6 ± 0.79	38.6 ± 0.61	22.0 ± 1.09
S. verruculosum		50.5 ± 1.78	27.2 ± 0.23	20.0 ± 0.44	34.5 ± 0.55	14.5 ± 0.89
ANOVA	*P*-value	< 0.01	< 0.01	< 0.01	< 0.01	< 0.01
	f-value	42.20	5.86	6.50	37.53	31.08

Table 1. Comparison of mean extracted parameters ($rETR_{max}$, T-opt, T-min, T-max and thermal range) from a Gaussian thermal performance curve for $rETR_{max}$ of four different taxa (*A. kenti, A. marina, U. lactuca* and *S. verriculosum*) across a thermal gradient (14–38.6 °C). Mean and standard error (SE) are reported for each parameter ($n = 4$). One-way Analysis of Variance (ANOVA) results are reported for Gaussian model outputs for each parameter to identify significant differences between taxa ($P < 0.05$). Full list of Tukey's post-hoc results can be found in Supplementary Table 3.

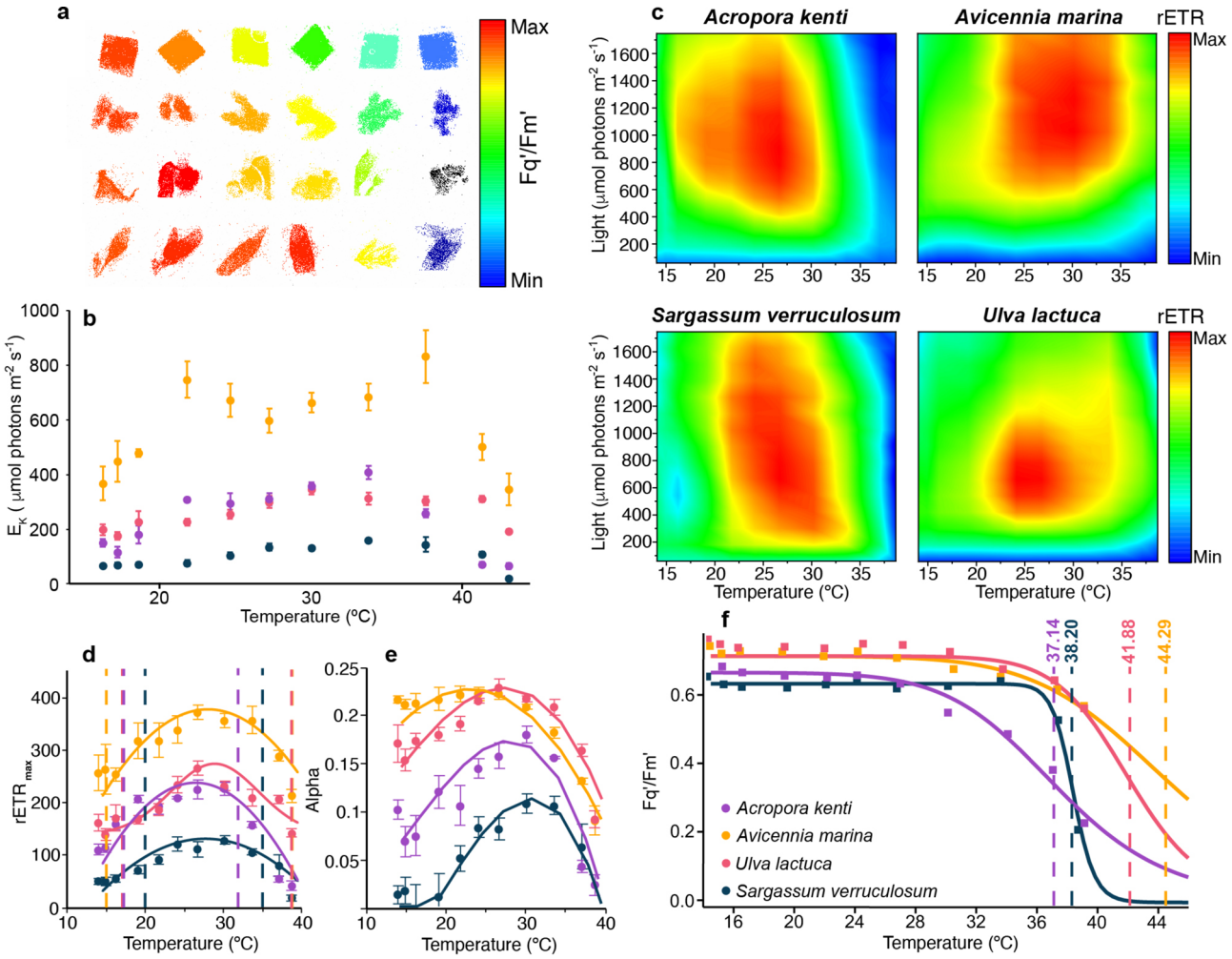

Fig. 2. Multi-taxa data collected using the MTP system *Protocol 1*. (**a**) Composite image of four taxa (in rows from top to bottom; *A. marina, A. kenti, U. lactuca* and *S. verruculosum*) showing effective quantum yield of PSII (F_q'/F_m') values across a temperature gradient (left to right) taken at T3 (see *Protocol 1* in Fig. 1b). (**b**) Scatter plot showing E_K values for *A. kenti, A. marina, U. lactuca* and *S. verruculosum* across a temperature gradient (14 °C to 38.6 °C). $n = 4$ per data point with standard error of mean shown. (**c**) Heatmaps showing relative electron transfer rates (rETR) across a gradient of light intensities and temperatures for the four taxa. (**d**) Maximum rETR values recorded during the RLC ($n = 4$, plots show mean ± standard error). Dashed lines indicate T-min and T-max values. (**e**) Alpha (α) values determined from the RLC ($n = 4$, plots show mean ± standard error). (**f**) F_q'/F_m' values recorded at T3 on *Protocol 1* with dashed lines indicating ED50 values for each taxon ($n = 4$ biological replicates).

Coral oxygen dynamics across a thermal gradient—P_G:R for all three species were highest at 26 °C before all falling below one at 35 °C (Fig. 4a–c; Supplementary Table 2). Both *M. capricornis* and *M. digitata* exhibited higher mean P_G:R (4.72 and 4.81) than *P. damicornis* (3.39) at 26 °C ($n = 8$). Average rETR values reached a maximum for *M. capricornis* and *P. damicornis* at 26 °C and 32 °C for *M. digitata* (Fig. 4d). Respiration rates (R) generally increased with temperature for all species (Fig. 4e) and were highest at 35 °C for *M. capricornis* and *M. digitata* compared to 26 °C for *P. damicornis*. There was a strong correlation between R and P_G at 15 °C ($r = 0.95$, $P = 0.001$), 26 °C ($r = 0.95$, $P = 0.001$), 32 °C ($r = 0.96$, $P = 0.001$) and 35 °C ($r = 0.98$, $P = 0.001$). Values of P_G were highest for all three species at 26 °C before rapidly declining at 35 °C. P_G for all species was directly compared to average rETR values across a temperature gradient of 15–35 °C (Fig. 4g). Both *M. capricornis* and *P. damicornis* showed correlation between P_G and rETR ($r = 0.68$, $P < 0.05$ and $r = 0.69$, $P < 0.05$), but less correlation occurred

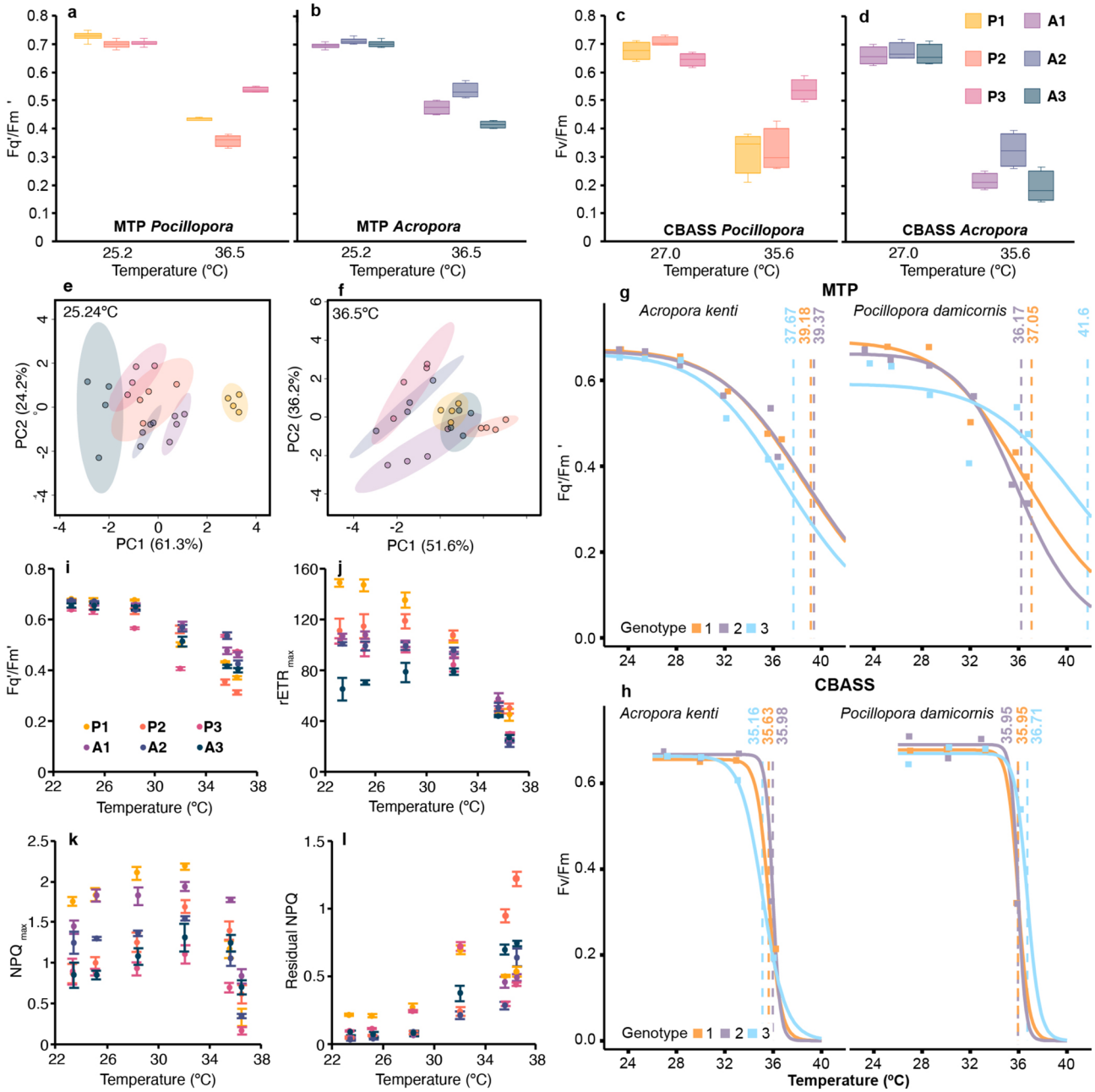

Fig. 3. Phenotypic differences in photophysiological parameters extracted from corals using the MTP system. Photophysiological parameters are presented for two species ($n = 3$ genotypes) *P. damicornis* (P1, P2, P3) and *A. kenti* (A1, A2, A3) across a temperature gradient. (a and b) Photosynthetic efficiency of PSII for *P. damicornis* and *A. kenti* when exposed to 25.2 °C and 36.5 °C for MTP (taken from T3, *Protocol 1*) and (c and d) for CBASS at 27.0 °C and 35.6 °C. (e and f) Principal Component Analysis (PCA) plots incorporating F_q'/F_m', $rETR_{max}$, α, NPQ_{max} and residual NPQ values across two different temperatures; groupings of the same genotype are depicted by coloured ovals. (i–l) show genotype data presented as mean ± standard error ($n = 4$ replicates per temperature). (i) F_q'/F_m' values taken from T3. (j) $rETR_{max}$ values taken during the rapid light curve. (k) NPQ_{max} values taken during the rapid light curve. (l) Residual NPQ values from T3. (g and h) Log logistic regression models fitted for each species (*P. damicornis* and *A. kenti*) for the MTP system and CBASS ($n = 4$ replicates per temperature point).

for *M. digitata* (r = 0.36). Higher P_G:R correlated with higher rETR values across the four temperatures (r = 0.63, $n = 96$, $P < 0.05$; Fig. 4h) with the highest rates for both parameters occurring at 26 °C and the lowest at 35 °C. The rETRs were highest at 26 °C for *M. capricornis* and *P. damicornis*, compared to at 32 °C for *M. digitata*.

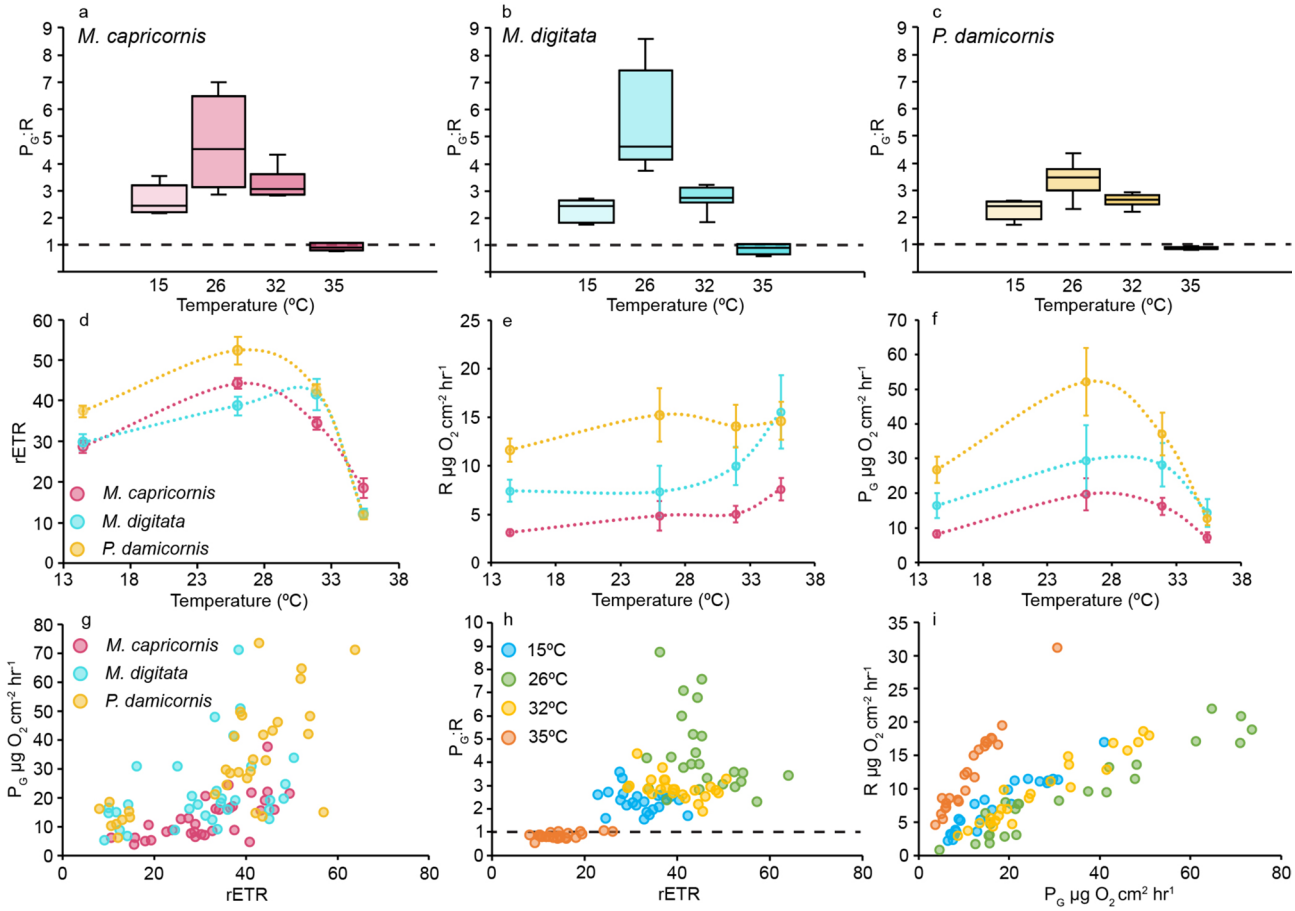

Fig. 4. Retrieved oxygen dynamics. (**a**–**c**) Gross photosynthesis to respiration (P_G:R) ratios across four temperatures for each species (*M. capricornis, M. digitata* and *P. damicornis)*. The dashed lines indicate a value of 1, below which metabolic needs are no longer met from primary production. Box plots show mean as the horizontal line, and upper and lower quartiles, with whiskers indicating maximum and minimum values. $n = 8$ replicates were used per species at each temperature. (**d**) Average rETR values from three different species (*M. capricornis, M. digitata* and *P. damicornis* were assessed using *Protocol 2* at 15, 26, 32 and 35 °C and 280 µmol photons m^{-2} s^{-1}. Dotted lines indicate 3rd order polynomials. (**e**) Average respiration rates (R; µg O_2 cm^{-2} h^{-1}) measured using *Protocol 2* under 30 min of darkness across different temperatures. (**f**) Average rates of gross photosynthesis (P_G; µg O_2 cm^{-2} h^{-1}) obtained using *Protocol 2* under 30 min of 280 µmol photons m^{-2} s^{-1} of light across different temperatures. (**g**) The relationship between gross photosynthesis (P_G) and mean rETR for each species ($n = 32$). (**h**) The relationship between gross photosynthesis (P_G) to respirations rates (P_G:R) and mean rETR values at different temperatures for all three corals combined ($r = 0.63$, $n = 96$, $P < 0.05$). (**i**) The relationship between respiration (R) and gross photosynthesis (P_G) for all species across four different temperatures ($n = 24$).

Discussion

International commitments to restore nature, such as the Kunming-Montreal Global Biodiversity Framework, are resulting in intensifying efforts to repair degraded ecosystems[35], but these restoration efforts are occurring within the context of intensifying climate change[36]. Thus, to maximise the success of restoration efforts, decisions need to be made on which taxa are chosen[37] as well as which areas are prioritised for restoration[38]. In terrestrial systems, high throughput phenotyping has been one tool assisting the decision making process[20,21], and more recent examples such as CBASS are being applied in marine ecosystems[22,23]. Here we describe a new system, comprised of three pieces of laboratory equipment customised to work together to retrieve a wealth of physiological parameters across user defined gradients.

In this manuscript we described the design, optimisation and implementation of the MTP system to identify differences in thermal performances both within and across different taxa. When designing and optimising the MTP system we undertook numerous validation steps centred around the integration of existing technologies to a single portable system. These included establishing the thermocycler protocols and undertaking thermal mapping of the MTP plate (Supplementary Fig. 2). Adaptability of the thermocycler temperature settings enables users to define target temperatures within the bounds of the thermocycler range. In order to increase the range and resolution of retrieved thermal performance curves (TPCs), multiple MTP runs can be performed. We further validated the integration of optical O_2 sensing and PAM fluorometry (Supplementary Fig. 7) and assessed the effect of well size and sample biomass on O_2 dynamics (Supplementary Fig. 7). As recommended by previous

incubation studies[28], measuring O_2 drawdown rates prior to application of the MTP system is recommended to optimise material biomass to the well plate volume. O_2 production and drawdown rates may vary from a variety of factors (e.g., by taxa, handling procedures and environmental history[39]) making it inappropriate to prescribe a set material size. One challenge with the current system is the absence of flow within the wells, meaning that there is no external disruption of sample boundary layers that could affect rate measurements. Recent research, however, has uncovered that coral has the capability to augment the mixing of O_2 in their lower boundary layer by utilising the movement of their cilia. This occurs independently of external flow speeds, demonstrating that flow alone does not determine how the boundary layer is disrupted[40]. Additionally, a recent study utilising similar well volumes and designs also did not incorporate flow or mixing within the wells when assessing O_2 dynamics of macroalgae[41]. Our data indicated immediate responses in O_2 levels to shifts between darkness and light (see Supplementary Figs. 7, 8) within the current protocol durations. Since all runs of the MTP protocol lacked flow, it ensured standardised conditions. However, it's important to exercise caution when extrapolating rates derived from the MTP system to other studies that incorporated flow.

The MTP system has customisable (e.g., temperature, time, light) protocols based on user needs, but two specific protocols were established for our current study: *Protocol 1*—A Multistage Dynamic Photophysiological Response Protocol and *Protocol 2*—An Oxygen Dynamic Response Protocol. The various stages of *Protocol 1* enabled application of numerous interacting abiotic variables to better predict how taxa will respond to future conditions[13]. Importantly, *Protocol 1* incorporated a dark–light-dark sequence to minimise O_2 depletion in the wells (Fig. 1b). *Protocol 1* was designed around incorporation of a Rapid Light Curve (RLC) approach that is commonly used in photophysiological research. RLCs provide valuable insights into the light-dependent processes and efficiencies of photoautotrophic activity by rapidly modulating light intensities and measuring the corresponding changes in photochemical activity[42]. Preliminary analysis on corals identified that an optimum light step length of 30 s was required to ensure $rETR_{max}$ remained high whilst inducing non-photochemical quenching within the samples (Supplementary Fig. 5). Low-light pre-illumination at 10 µmol photons m^{-2} s^{-1} was included in the stages between measurements of the protocol to ensure all samples were at the same light state as well as to counteract the effects of dark acclimation (restriction of the Calvin cycle and consumption of ATP and NADPH), prime the photosystems and mimic natural conditions. The use of pre-illumination was also decided upon out of a consideration of practicality and reproducibility. Dark acclimated F_v/F_m measurements taken by hand with instruments such as the Walz diving PAM require the user to be able to see the samples, implying that there is generally always some amount of light surrounding the samples. This stray light is often overlooked and has the potential to influence the measurements that are taken. The ability to completely dark acclimate a sample for a F_v/F_m measurement is not always possible, especially when undertaking field work with varying light conditions. By adding a constant, yet small amount of pre-illumination both before and during the PAM measurement, accuracy and reproducibility of specific lighting conditions can be ensured. Notably, this aspect of the protocol is user defined, and can be changed as required.

Protocol 2—An Oxygen Dynamic Response Protocol can provide unique insight into holobiont physiology beyond standard photochemistry metrics[31,43]. While O_2 readings can be extracted during *Protocol 1*, longer incubation times were necessary at given light intensities (e.g., dark versus light) to extract O_2 dynamics that could be used to quantify useful descriptions of metabolic rates (e.g., net photosynthesis and respiration rates). Optical O_2 sensors (see methods) are widely utilised[30,44], including in conjunction with other chlorophyll *a* fluorescence-based methods such as the Walz diving PAM[31]. In integrating O_2 sensing, the MTP system therefore can retrieve absolute rates of net photosynthesis and respiration, although this requires time-consuming and separate semi-continuous calibration (see methods) and sample-specific surface area normalisation[28]. We therefore propose using P_G:R (gross photosynthesis to respiration ratio) since it is a self-normalising value to retain the MTP high throughput capacity.

Coral oxygen dynamics across a thermal gradient—O_2 consumption rates are a critical measure of energy metabolism and a vital indicator of mitochondrial health and therefore overall cellular regulation or dysfunction[43]. The ability of the MTP system to measure high-throughput O_2 dynamics across environmental gradients provides valuable insights into the overall health and functionality of complex organisms such as coral holobionts, where one photobiological metric may be limited in explaining the intricate relationship between the heterotrophic coral host and its autotrophic algal symbionts and how it affects phenotypic performance[45]. Inclusion of O_2 sensing alongside fluorometry in the MTP system broadens our capacity for a physiological assessment of entire organisms, and thus holobiont (or metaorganism) phenotyping. Rates of P_G were highest for all three species at 26 °C before rapidly declining at 35 °C, indicating downregulation and/or photoinhibition of PSII apparatus[46]. P_G:R for all three species were highest at 26 °C before all falling below one at 35 °C (Supplementary Table 2), indicating a shift in their metabolic activities away from being primarily autotrophic to heterotrophic[47]. Both *M. capricornis* and *M. digitata* exhibited higher mean P_G:R (4.72 and 4.81) than *P. damicornis* (3.39) at 26 °C ($n = 8$), indicating that *M. capricornis* and *M. digitata* met more of their metabolic requirements through photosynthetic activity[46] than *P. damicornis*. Further, we observed that higher O_2 production correlated with higher rETR across all species, an outcome in agreement with prior studies that similarly showed good linear correlation between photosynthetic rates measured via chlorophyll *a* fluorescence and O_2[48,49]. However, under higher temperatures this correlation broke down, indicating an offset between P_G and rETR which can be caused by a shift in electron distribution, giving an indication of how much P_G O_2 is being recycled via alternative electron pathways such as the Melher reaction[50,51], and thus providing important information on tolerance thresholds[45]. Rates of P_G and R for all corals (Fig. 4i) showed a strong correlation across all temperatures, indicating that metabolic rates are similarly governed by temperature for all coral[52].

Multi-taxa comparison—Our results showed that *A. kenti* exhibited lower thermal tolerance than other taxa sampled, supporting previous work on coral exhibiting lower thermal tolerance than marine algae and plants[53,54]. TPCs have been extensively applied to establish the breadth and optimum temperature performance for some

marine taxa more (e.g., marine algae[55]) than others (e.g., coral[56]). Multiple modelling approaches have been applied across TPC studies[33,34], and model suitability varies depending on the input parameter[33,57]. Heatmaps for $rETR_{max}$ from all four taxa (Fig. 2c) were created to visualise how photochemical capacity changed with temperature and light interactions, revealing species-specific responses, and hence insight into, specific environmental niche spaces. Notably, the ranking of taxa performance based on T-opt for α was different to that of T-opt for $rETR_{max}$, which was unsurprising given they describe different aspects of how photochemical efficiency is governed by light availability. Together these metrics can also provide unique insights into the thermal niche of an organism as well as an indication that such reductions in photosystem capacity and efficiency due to thermal stress could be a good indicator of photosystem downregulation or damage. For example, *A. kenti* T-opt for $rETR_{max}$ was 24.7 °C, while T-opt for α was 27.5 °C suggesting efficient photochemistry is sustained under higher temperatures when light is limiting. Previous work has also demonstrated differences in TPCs based on the parameter used; it is thus important for users of the MTP system to select appropriate parameters to model TPCs dependent on their research question[57]. Other parameters retrieved from *Protocol 1*—(Fig. 3i–l) not used for TPCs can still provide important information on taxa environmental history; for example, E_K (the minimum saturating light intensity) reflects the light history of an organism[58]. E_K values for all taxa were highly variable with temperature (Fig. 2b), highlighting the need to account for temperature history in parallel when describing E_K. Collectively the multi-taxa comparison using the MTP system (*Protocol 1*) identified differences in photophysiological performance across temperatures, but in alignment with previous studies, and where phenotypic ranking varies depending on the parameter used[57]. Taxa with smaller thermal niches have the potential to be more impacted by climate change[59]; thus, understanding predicted thermal niches can support conservation planning and has been highlighted as a research priority, particularly for marine taxa[26]. However, future consideration is needed to validate how the MTP predicted thermal responses reflect observed thermal niches in the environment.

MTP and CBASS derived phenotypes—Conceptually, MTP and CBASS are similar in that both systems can be utilised to test thermal performance across a defined temperature range (although MTP is more centred around thermal optima, whereas CBASS is more centred around thermal limits). The MTP approach differs from CBASS in that it is a much faster assay, assesses a broader range of temperatures, and retrieves a suite of photophysiological parameters to create a thermal performance curve (Fig. 3i–l). The 18-h CBASS assay allows for assessment of two distinct parameters: (i) heat stress response (after 7 h, directly following the heat-hold) and (ii) recovery response (after 18 h, following an overnight reprieve). The difference between the 7-h and 18-h responses can provide insight into putative resilience potential (e.g., some corals exhibit recovery of F_v/F_m after 18 h, while others further lose photosynthetic efficiency). Studies using the CBASS approach typically use a PAM (Walz, Germany) to capture F_v/F_m (maximum dark acclimated photochemical efficiency) as the photophysiological response parameter, although any continuous variable can be used for the purpose of thermal threshold modelling, such as coral whitening, protein biomass, or similar[22]. Modelling of CBASS response variables are used to determine the temperature at which a 50% reduction of the trait under consideration (e.g., F_v/F_m or colour) occurs (reported as the ED50 thermal tolerance threshold[21,22]). One important consideration when applying the same CBASS models to MTP data is that if observed photochemical efficiency does not drop significantly enough (e.g., temperature exposures were not high enough to elicit at least a 50% decline in the test parameter) to capture the ED50 value, it will be predicted rather than observed.

Whilst F_v/F_m (CBASS) and F_q'/F_m' (MTP) are both measures of photosystem efficiency, F_v/F_m is a measure of maximum dark-acclimated efficiency and F_q'/F_m' is a measure of light acclimated efficiency (Supplementary Table 6). These photophysiological nuances do not allow for a direct comparison in photochemical results, rather a broader comparison of observed phenotypes. Despite fundamental differences in the two methods, the phenotypic response patterns were generally the same across both systems, suggesting that shorter timeframes (e.g., 45 min (MTP) versus 18 h (CBASS)) may be suitable to capture acute thermal stress response phenotypes. Values of ED50 from the CBASS were generally lower, however, than those from the MTP, most likely reflecting more accumulated stress from longer experimental time of the CBASS. Notably, both the CBASS and MTP methods expose taxa to acute heat stress, and such a short experimental assay time may not always be sufficient to accurately depict organismal responses to environmental stressors over longer time periods[60]. However, the use of MTP and other analogues[22,23] rapidly provide users with valuable information on the overall health and potential resilience of an organism when exposed to environmental change. Whilst recent work[24] has shown good correlation between CBASS predicted and real world observed phenotypic performance, further testing is required downstream to verify this link. Additionally, while the equipment used (Imaging PAM and thermocycler) are standalone items available for laboratories, their cost could make the MTP system prohibitive, and therefore custom built, low-cost variations should be considered in the future.

Conclusion

This paper demonstrates the potential value of high-throughput phenotyping systems, such as the MTP system, to advance knowledge on the responses of key aquatic organisms to environmental change, thus providing a powerful and much needed tool to research, restoration and industry stakeholders. We acknowledge that the MTP system could be cost-prohibitive for some end-users, so further efforts to customise cheaper versions that overcome limits of the current system (e.g., no flow) is an area for further development. The MTP system combination of portability and high throughput capacity across defined conditions allows for the extraction of a wide range of physiological parameters, providing insights into aquatic organism functioning across varying and predicted environmental conditions. Further, we provide a series of protocols which other researchers can tailor to suit their target taxa and research questions. Whilst this device has shown strong potential in predicting taxon and phenotype specific thermal performance, future studies validating how rapid phenotyping tools such

as the MTP system predict phenotypic responses to long term environmental changes in situ are needed to fully understand the value of rapid-assay phenotyping.

Data availability

All data is included within this manuscript or supplementary materials.

Code availability

All code used within the manuscript is available https://github.com/HadleyEngland.

Received: 6 February 2024; Accepted: 2 September 2024
Published online: 18 September 2024

References

1. Hughes, T. P. *et al.* Coral reefs in the Anthropocene. *Nature* **546**, 82–90 (2017).
2. Wernberg, T. *et al.* Climate-driven regime shift of a temperate marine ecosystem. *Science* **353**, 169–172 (2016).
3. Hoegh-Guldberg, O., Poloczanska, E. S., Skirving, W. & Dove, S. Coral reef ecosystems under climate change and ocean acidification. *Front. Mar. Sci.* **4**, 158 (2017).
4. Koch, M., Bowes, G., Ross, C. & Zhang, X.-H. Climate change and ocean acidification effects on seagrasses and marine macroalgae. *Glob. Change Biol.* **19**, 103–132 (2013).
5. Fiehn, O. Metabolomics—The link between genotypes and phenotypes. *Plant Mol. Biol.* **48**, 155–171 (2002).
6. Arbona, V., Manzi, M., de Ollas, C. & Gómez-Cadenas, A. Metabolomics as a tool to investigate abiotic stress tolerance in plants. *Int. J. Mol. Sci.* **14**, 4885–4911 (2013).
7. Houle, D., Govindaraju, D. R. & Omholt, S. Phenomics: The next challenge. *Nat. Rev. Genet.* **11**, 855–866 (2010).
8. Suggett, D. J. *et al.* Toward bio-optical phenotyping of reef-forming corals using light-induced fluorescence transient-fast repetition rate fluorometry. *Limnol. Oceanogr. Methods* **20**, 172–191 (2022).
9. Bhagooli, R. *et al.* Chlorophyll fluorescence—A tool to assess photosynthetic performance and stress photophysiology in symbiotic marine invertebrates and seaplants. *Mar. Pollut. Bull.* **165**, 112059 (2021).
10. Hoadley, K. D. *et al.* A phenomic modeling approach for using chlorophyll-a fluorescence-based measurements on coral photosymbionts. *Front. Mar. Sci.* https://doi.org/10.3389/fmars.2023.1092202 (2023).
11. Murchie, E. H. *et al.* Measuring the dynamic photosynthome. *Ann. Bot.* **122**, 207–220 (2018).
12. Suggett, D. J. & Prášil, O. *Chlorophyll a Fluorescence in Aquatic Sciences: Methods and Applications* (Springer, 2010). https://doi.org/10.1007/978-90-481-9268-7.
13. Herdean, A., Sutherland, D. L. & Ralph, P. J. Phenoplate: An innovative method for assessing interacting effects of temperature and light on non-photochemical quenching in microalgae under chemical stress. *New Biotechnol.* **66**, 89–96 (2022).
14. Xiao, L. *et al.* Photophysiological response of Symbiodiniaceae single cells to temperature stress. *ISME J.* **16**, 2060–2064 (2022).
15. Summers, N., Fragoso, G. M. & Johnsen, G. Photophysiologically active green, red, and brown macroalgae living in the Arctic Polar Night. *Sci. Rep.* **13**, 17971 (2023).
16. Barott, K. *et al.* Hyperspectral and physiological analyses of coral-algal interactions. *PLoS One* **4**, e8043 (2009).
17. Herdean, A. *et al.* Temperature mapping of non-photochemical quenching in *Chlorella vulgaris*. *Photosynth. Res.* **155**, 191–202 (2023).
18. Quaas, T. *et al.* Non-photochemical quenching and xanthophyll cycle activities in six green algal species suggest mechanistic differences in the process of excess energy dissipation. *J. Plant Physiol.* **172**, 92–103 (2015).
19. Cruz, J. A. *et al.* Dynamic environmental photosynthetic imaging reveals emergent phenotypes. *Cell Syst.* **2**, 365–377 (2016).
20. Yang, W. *et al.* Crop phenomics and high-throughput phenotyping: Past decades, current challenges, and future perspectives. *Mol. Plant* **13**, 187–214 (2020).
21. Fernández-Calleja, M. *et al.* Rapid on-site phenotyping via field fluorimeter detects differences in photosynthetic performance in a hybrid—Parent barley germplasm set. *Sensors* **20**, 1486 (2020).
22. Voolstra, C. R. *et al.* Standardized short-term acute heat stress assays resolve historical differences in coral thermotolerance across microhabitat reef sites. *Glob. Change Biol.* **26**, 4328–4343 (2020).
23. Evensen, N. R. *et al.* The Coral Bleaching Automated Stress System (CBASS): A low-cost, portable system for standardized empirical assessments of coral thermal limits. *Limnol. Oceanogr. Methods* **21**, 421–434 (2023).
24. Klepac, C. N. *et al.* Assessing acute thermal assays as a rapid screening tool for coral restoration. *Sci. Rep.* **14**, 1898 (2024).
25. Goulet, T. L., Erill, I., Ascunce, M. S., Finley, S. J. & Javan, G. T. Conceptualization of the holobiont paradigm as it pertains to corals. *Front. Physiol.* **11**, 566968 (2020).
26. Camp, E. F. Contingency planning for coral reefs in the Anthropocene; The potential of reef safe havens. *Emerg. Top. Life Sci.* **6**, 107–124 (2022).
27. Hennige, S. J. *et al.* Photoacclimation, growth and distribution of massive coral species in clear and turbid waters. *Mar. Ecol. Prog. Ser. Halstenbek* **369**, 77–88 (2008).
28. Camp, E. F. *et al.* The "Flexi-Chamber": A novel cost-effective in situ respirometry chamber for coral physiological measurements. *PLoS One* **10**, e0138800 (2015).
29. McLachlan, R. H. & Grottoli, A. G. Geometric method for estimating coral surface area using image analysis. *Protocolsio* https://doi.org/10.17504/protocols.io.bpxcmpiw (2021).
30. Sukigara, C. *et al.* Measurement of oxygen concentrations and oxygen consumption rates using an optical oxygen sensor, and its application in hypoxia-related research in highly eutrophic coastal regions. *Cont. Shelf Res.* **229**, 104551 (2021).
31. Hughes, D. J. *et al.* Widespread oxyregulation in tropical corals under hypoxia. *Mar. Pollut. Bull.* **179**, 113722 (2022).
32. Sorek, M., Yacobi, Y. Z., Roopin, M., Berman-Frank, I. & Levy, O. Photosynthetic circadian rhythmicity patterns of Symbiodium, the coral endosymbiotic algae. *Proc. R. Soc. B Biol. Sci.* **280**, 20122942 (2013).
33. Padfield, D., O'Sullivan, H. & Pawar, S. rTPC and nls.multstart: A new pipeline to fit thermal performance curves in r. *Methods Ecol. Evol.* **12**, 1138–1143 (2021).
34. Angilletta, M. J. Estimating and comparing thermal performance curves. *J. Therm. Biol.* **31**, 541–545 (2006).
35. Suggett, D. J. *et al.* Restoration as a meaningful aid to ecological recovery of coral reefs. *Npj Ocean Sustain.* **3**, 1–4 (2024).
36. AR6 Synthesis Report: Climate Change 2023. https://www.ipcc.ch/report/ar6/syr/.
37. Butt, N. & Gallagher, R. Using species traits to guide conservation actions under climate change. *Clim. Change* **151**, 317–332 (2018).
38. Strassburg, B. B. N. *et al.* Global priority areas for ecosystem restoration. *Nature* **586**, 724–729 (2020).
39. Camp, E. F. *et al.* Mangrove lagoons of the Great Barrier Reef support coral populations persisting under extreme environmental conditions. *Mar. Ecol. Prog. Ser. Halstenbek* **625**, 1–14 (2019).
40. Pacherres, C. O., Ahmerkamp, S., Schmidt-Grieb, G. M., Holtappels, M. & Richter, C. Ciliary vortex flows and oxygen dynamics in the coral boundary layer. *Sci. Rep.* **10**, 7541 (2020).

41. Veenhof, R. J. *et al.* Novel high-throughput oxygen saturation measurements for quantifying the physiological performance of macroalgal early life stages. *J. Phycol.* n/a.
42. Ralph, P. J. & Gademann, R. Rapid light curves: A powerful tool to assess photosynthetic activity. *Aquat. Bot.* **82**, 222–237 (2005).
43. Brito, M. D. *et al.* Oxygen consumption evaluation: An important indicator of metabolic state, cellular function cellular function, and cell fate along neural deregulation neural deregulation. In *Toxicity Assessment: Methods and Protocols* (eds Palmeira, C. M. M. *et al.*) 207–230 (Springer, 2021). https://doi.org/10.1007/978-1-0716-1091-6_15.
44. Castrillón-Cifuentes, A. L., Zapata, F. A., Giraldo, A. & Wild, C. Spatiotemporal variability of oxygen concentration in coral reefs of Gorgona Island (Eastern Tropical Pacific) and its effect on the coral *Pocillopora capitata*. *PeerJ* https://doi.org/10.7717/peerj.14586 (2023).
45. Suggett, D. J. *et al.* Sea anemones may thrive in a high CO_2 world. *Glob. Change Biol.* **18**, 3015–3025 (2012).
46. Mathur, S., Agrawal, D. & Jajoo, A. Photosynthesis: Response to high temperature stress. *J. Photochem. Photobiol. B* **137**, 116–126 (2014).
47. Hoogenboom, M., Rodolfo-Metalpa, R. & Ferrier-Pagès, C. Co-variation between autotrophy and heterotrophy in the Mediterranean coral *Cladocora caespitosa*. *J. Exp. Biol.* **213**, 2399–2409 (2010).
48. Ben-Zvi, O. *et al.* Photophysiology of a mesophotic coral 3 years after transplantation to a shallow environment. *Coral Reefs* **39**, 903–913 (2020).
49. Trampe, E., Hansen, P. J. & Kühl, M. A comparison of photosynthesis measurements by O2 evolution, 14C assimilation, and variable chlorophyll fluorescence during light acclimatization of the diatom *Coscinodiscus granii*. *Algae Korean Phycol. Soc.* **30**, 103–119 (2015).
50. Roberty, S., Bailleul, B., Berne, N., Franck, F. & Cardol, P. PSI Mehler reaction is the main alternative photosynthetic electron pathway in *Symbiodinium* sp., symbiotic dinoflagellates of cnidarians. *New Phytol.* **204**, 81–91 (2014).
51. Roberty, S. *et al.* Shallow and mesophotic colonies of the coral Stylophora pistillata share similar regulatory strategies of photosynthetic electron transport but differ in their sensitivity to light. *Coral Reefs* **42**, 645–659 (2023).
52. Sawall, Y., Nicosia, A. M., McLaughlin, K. & Ito, M. Physiological responses and adjustments of corals to strong seasonal temperature variations (20–28 °C). *J. Exp. Biol.* **225**, jeb244196 (2022).
53. Li, X. *et al.* Correlations between photosynthetic heat tolerance and leaf anatomy and climatic niche in Asian mangrove trees. *Plant Biol. Stuttg. Ger.* **24**, 960–966 (2022).
54. Anton, A. *et al.* Differential thermal tolerance between algae and corals may trigger the proliferation of algae in coral reefs. *Glob. Change Biol.* **26**, 4316–4327 (2020).
55. Baker, K. G. *et al.* Thermal performance curves of functional traits aid understanding of thermally induced changes in diatom-mediated biogeochemical fluxes. *Front. Mar. Sci.* https://doi.org/10.3389/fmars.2016.00044 (2016).
56. Jurriaans, S. & Hoogenboom, M. O. Seasonal acclimation of thermal performance in two species of reef-building corals. *Mar. Ecol. Prog. Ser. Halstenbek* **635**, 55–70 (2020).
57. Dilernia, N. J., Camp, E. F., Bartels, N. & Suggett, D. J. Contrasting the thermal performance of cultured coral endosymbiont photo-physiology. *J. Exp. Mar. Biol. Ecol.* **561**, 151865 (2023).
58. Sakshaug, E. *et al.* Parameters of photosynthesis: Definitions, theory and interpretation of results. *J. Plankton Res.* **19**, 1637–1670 (1997).
59. Sunday, J. M., Bates, A. E. & Dulvy, N. K. Thermal tolerance and the global redistribution of animals. *Nat. Clim. Change* **2**, 686–690 (2012).
60. Rosenqvist, E., Großkinsky, D. K., Ottosen, C.-O. & van de Zedde, R. The Phenotyping dilemma—The challenges of a diversified phenotyping community. *Front. Plant Sci.* **10**, 163 (2019).

Acknowledgements

The authors extend their thanks to Mr John Edmondson of Wavelength Reef Cruises for his support collecting material for testing.

Author contributions

H.E., A.H., E.F.C. conceived the project with input from C.R.V. and D.J.S. H.E. and A.H. led the code concept and H.E., A.H. and E.F.C. undertook the testing and optimisation of the set up. H.E. visualised data and prepared the figures. E.F.C., J.M., and A.H. supervised the project. H.E., A.H. and E.F.C. led the writing, with input and editing from C.R.V., D.J.S., J.M., D.J.H. and C.D.R. E.F.C. acquired the funding and administered the project.

Funding

Funding of this work was supported from a Philanthropic Donation of David and Susan Rockefeller to EFC.

Competing interests

The authors declare no competing interests.

Additional information

Supplementary Information The online version contains supplementary material available at https://doi.org/10.1038/s41598-024-71972-5.

Correspondence and requests for materials should be addressed to H.E. or E.F.C.